RESEARCH PAPER

Mechanical Properties and Electrical Conductivity of Poly(methyl methacrylate)/Multi-walled Carbon Nanotubes Composites

Nadia A. Ali[1] · Seenaa I. Hussein[1] · Tesleem B. Asafa[2] · Alaa M. Abd-Elnaiem[3]

Abstract

Carbon nanotubes (CNTs) remain one of the most efficient reinforcing material for enhanced mechanical and electrical properties. In this study, the effects of multi-walled CNTs (MWCNTs) fillers on mechanical, structural, and electrical properties of polymethyl methacrylate (PMMA)/MWCNTs composites were studied. The PMMA/MWCNTs composites, containing varying MWCNTs concentration of 0.1, 0.3, and 0.5 wt%, were prepared by a solution casting method. The mechanical properties of the composites such as tensile strength, elongation, Young modulus, tear resistance, fracture energy, impact strength, and hardness were investigated. Results showed that the mechanical properties of the composites were enhanced significantly. At 0.5 wt% MWCNTs, the tensile strength, elongation, tear strength, hardness, fracture energy and impact strength increased by 397%, 567%, 89%, 27%, 12%, and 36%, respectively, while the Young modulus decreased by 26% compared to pure PMMA polymer sample. Both the dc electrical conductivity and the activation energy increased with increased concentration of MWCNTs. From the electrical conductivity measurements, the percolation threshold was found to equal ∼ 0.55 wt% MWCNTs. Based on the Fourier-transform infrared spectroscopy analysis, enhancement of mechanical and electrical properties is attributed to the formation of covalent bonds between polymer strands and MWCNTs. Moreover, a mechanism was proposed to describe the influence of MWCNTs on electrical and mechanical properties of PMMA/MWCNTs composites.

Keywords PMMA · FTIR · MWCNTs · Tensile strength · Tear resistance · Hardness · Electric conductivity

1 Introduction

The application of polymers is on the rise due to their advantages over conventional materials (e.g., metals). Polymers are light in weight, corrosion-resistant, and are easily produced at low cost (Aguilar and San Román 2019; Khutoryanskiy and Georgiou 2018; Nezakati et al. 2018; Yuan et al. 2012). While several advancements have been made in polymer technology, their physical properties can be further enhanced by the addition of different fillers such as metal particles, semiconductors, organic and inorganic particles, carbon, ceramics and fibers among others (Abd-Elnaiem et al. 2020; Hussein et al. 2018; Prasher et al. 2006). Polymers modified with different fillers have enhanced structural, optical, thermal, electrical, mechanical and magnetic properties. This widens the scope of their applications ranging from structural units in the construction industry to aerospace and medical applications (Huang et al. 2003). Polymethyl methacrylate (PMMA), similar to other polymers, is transparent, compatible with the human body, has low weight, and possesses excellent optical clarity and good weathering behavior (Logakis et al. 2011). However, PMMA is brittle and insulating hence it cannot be deployed for applications where ductility or conductivity is an important consideration. Several studies have been conducted to enhance the mechanical properties of PMMA (Landry et al. 1992; Ash et al. 2002; Chen et al. 2007; Stipho 1998; Layek et al. 2010; Zhang et al. 2018; Pahlevanzadeh et al. 2019; Münker et al. 2018). Among

✉ Alaa M. Abd-Elnaiem
   abd-elnaiem@aun.edu.eg

[1] Department of Physics, College of Science, University of Baghdad, Baghdad, Iraq

[2] Department of Mechanical Engineering, Ladoke Akintola University of Technology, Ogbomoso, Oyo State, Nigeria

[3] Physics Department, Faculty of Science, Assiut University, Assiut 71516, Egypt

them are blending and copolymerization (Logakis et al. 2011) which have significantly enhanced the toughness of the polymer.

Multi-Walled Carbon Nanotubes (MWCNTs) are considered as one of the most important nano-reinforcing materials because of their high modulus (~ 1 TPa) and tensile strength (~ 63 GPa) emanated from the strong bonds between the carbon atoms (Meysami et al. 2017; Zhi et al. 2008; Huang et al. 2011; Deep and Mishra 2018; Mir et al. 2016; Faraguna et al. 2018; Mittal 2014). They have been widely deployed for reinforcement of polymer with enhanced physical and mechanical properties (Faraguna et al. 2018). The degree of enhancement depends on how well CNTs disperse in the matrix and the subsequent interfacial interactions between them. A study showed that the presence of 1 wt% MWCNTs improved the thermal stability and thermal conductivity of PMMA/MWCNTs composites (Deep and Mishra 2018). Blond et al. (2006) enhanced Young's modulus and strength of poly(vinyl alcohol) based composites by 3.7 and 3.9, respectively, by adding 1 wt% of CNTs. In this case, CNTs provide surfaces for better stress transfer. In the simulation results of Arash et al. (2014), the Young's modulus of PMMA/CNT polymer composite increased from 3.9 to 6.85 GPa when 5 wt% CNTs was incorporated. Mir et al. reported a higher electrical percolation threshold for PMMA/MWCNTs composites compared to other published data (Mir et al. 2016). The strengthening efficiency of MWCNTs can also be improved by coating the surfaces with surfactants or compatibilizers (Mittal 2014). Due to the interesting properties of the developed PMMA/MWCNTs composites, they are being deployed for several applications in aerospace, automobile, sports, bone-bonding ability, hydrogen gas permeation, electronics sectors among others (Münker et al. 2018; Nakason et al. 2005; Kumar et al. 2010; Yuen et al. 2008; Nawar and El-Mahalawy 2019; Su and Wang 2007; Wang et al. 2019).

Currently, limited reports on electrical and mechanical properties of PMMA/MWCNTs composites are available in the literature. The present investigation aims to extend the previous studies by investigating the influence of low concentrations (0–0.5 wt%) of MWCNTs on the mechanical and electrical properties of PMMA/MWCNTs composites synthesized by a solution casting method. Various mechanical parameters of the PMMA/MWCNTs composites such as tensile strength, elongation, tear resistance, fracture energy, impact strength, and hardness were investigated. Moreover, the electrical conductivity as a function of temperature was studied and the value of the percolation threshold was determined and discussed. In addition, a mechanism describing the influence of MWCNTs on electrical and mechanical properties of PMMA/MWCNTs composites was proposed.

2 Experimental Details

2.1 Materials

The PMMA (Mw $\sim 15{,}000$ by GPC) samples were obtained from Sigma-Aldrich Company while the MWCNTs (95%), having an outer diameter of 5–15 nm, inside diameter of 3–5 nm and length of 50 μm, were purchased from US Research nanomaterials, INC., Houston, USA.

2.2 Preparation of PMMA/MWCNTs Composites

The MWCNTs have grain size distribution within the range of 12–14 nm (Fig. 1). The preparation of the PMMA/MWCNTs composites followed the procedure depicted in Fig. 2a. Solution A was made from 2 g of pure PMMA dissolved in 10 ml of Chloroform ($CHCl_3$) and then stirred with a magnetic stirrer at 60 °C for 1 h to obtain a grade solution of PMMA. Similarly, solution B was prepared from MWCNTs dissolved in 10 ml of $CHCl_3$ and agitated ultrasonically at 30 °C for 10 min. Thereafter, solutions A and B were mixed and stirred vigorously for 1 h at 60 °C. The final mixture was then thoroughly sonicated until a stable, black-colored solution of PMMA/MWCNTs composite was formed. The PMMA/MWCNTs samples were prepared with 0.1, 0.3 and 0.5 wt% MWCNTs. They were then cast on the Petri dish and kept at 60 °C in an oven for 24 h to ensure the solvent was completely removed. The optical images of the prepared PMMA/MWCNTs thin sheet samples are presented in Fig. 2b. The PMMA sample without MWCNTs was considered as the control.
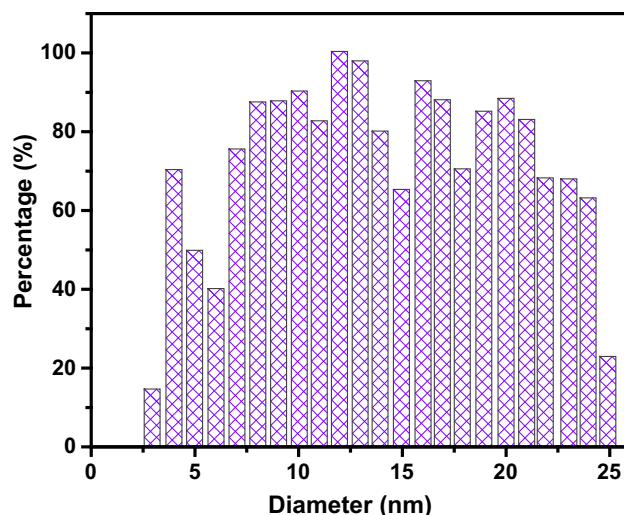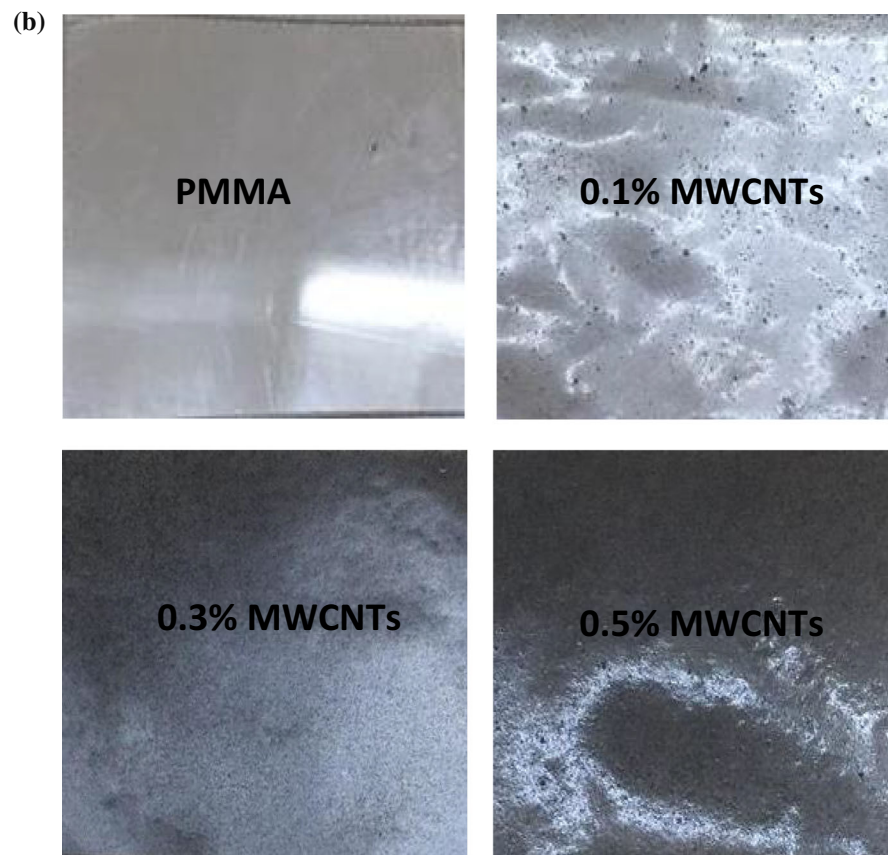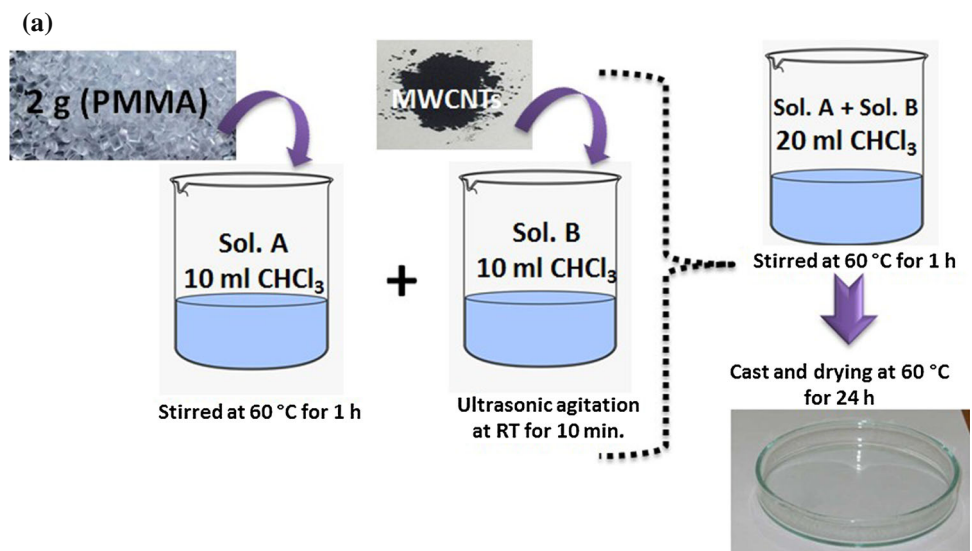

Fig. 1 Normal distribution histogram for MWCNTs nanoparticles

Fig. 2 a A schematic illustration of the fabrication procedure, and **b** optical images of the PMMA/MWCNTs composites (sample dimension is 2 cm × 2 cm)

(a)

(b)

2.3 Characterizations of PMMA/MWCNTs Composites

The thicknesses of the PMMA and PMMA/MWCNTs composites were measured with an electronic digital micrometer (IDM) of ± 0.001 sensitivity. The IDM cycled up and down automatically at the push of a button, providing an accurate and repeatable reading at the end of each cycle. The sheet samples were ∼ 115 μm thick.

The infrared spectra of the sheet samples were recorded with SHIMADZU FTIR-7600 in the range of 400–4000 cm^{-1}. The Fourier-transform infrared spectroscopy (FTIR) spectra gave information about the chemical structures of pure PMMA and PMMA/MWCNTs

composites. The surface morphology of the composites was investigated by JEOL JSM-5600LV scanning electron microscopy (SEM, Tokyo Japan). The SEM images were analyzed for the grain size and distribution using image processing software (ImageJ, Version 1.37).

The tensile test was conducted at room temperature ($\sim$ 30 °C) using Instron 4467 tensile tester following the ASTMD-882 standard (D882-18 2018). Sheet samples of dimensions 10 mm $\times$ 80 mm $\times$ 0.115 mm were tested at an extension rate of 5 mm/min while the Young modulus and tensile strength were obtained from the stress–strain curves. Tear resistance (tear strength) is another mechanical property associated with material failure and is normally quoted in terms of tear force per unit thickness N/mm (Kaufman 2001). Tear strengths of the samples were determined using Universal Electronic Dynamometer according to ASTM D-1922 standard. The sample (100 mm long by 60 mm wide) has 50 mm cut at the center. The experiments were conducted at 180 mm/min extension rate. A pendulum impact tester was used to measure the force required to propagate slit at a fixed distance to the edge of the test sample. Shore D hardness was conducted to measure the hardness of 170 mm $\times$ 10 mm $\times$ 4 mm sheet samples. Most of the numerical values of the mechanical properties were estimated by taking averages of three readings.

The Charpy impact test is a standardized high strain-rate test for measuring the amount of energy absorbed by a material during fracture. The test was conducted following ASTM D256 standard on bar-shaped specimens of dimension 170 mm $\times$ 10 mm $\times$ 4 mm). The Impact Strength (I.S.) was evaluated from Eq. (1):

$$\text{I.S.} = \frac{\text{F.E.} - 0.09\text{J}}{a \times b} \tag{1}$$

where F.E. is the fracture energy, a and b are the length and width of the tested sample, respectively.

The electrical resistivity (ρ) of the samples was measured within a temperature range of 303–393 K with the electrical measurement setup shown in Fig. 3 using Eq. (2):

$$\rho = \frac{RA}{L} \tag{2}$$

where R is the sample resistance (Ω), A is the cross-sectional area (mm^2) and L is the thickness of the specimen (mm). The PMMA/MWCNTs samples were 0.11 mm thick circular sheet of radius 0.55 cm. The dc electrical conductivity (σ_{dc}) was determined as the reciprocal of the resistivity using the following equation:

$$\sigma_{dc} = \frac{1}{\rho} \tag{3}$$

In addition, the activation energies for the conduction (E_a) were estimated from the plot of $\ln(\sigma)$ versus 1000/T according to the Arrhenius equation:

$$\sigma_{dc} = A_0 e^{\frac{-E_a}{k_B T}} \tag{4}$$

where k_B is the Boltzmann's constant (1.38×10^{-23} J/K) and A_0 is the pre-exponential factor.

3 Results and Discussions

The FTIR spectra of the pure PMMA sample, Fig. 4 curve (a), has absorption peaks around 2992 cm^{-1} and 2949 cm^{-1} corresponding to C–H asymmetric stretching in CH$_3$ and CH$_2$, respectively. The vibrational band at 2847 cm^{-1} is due to the C–H symmetric stretching in CH$_3$. The characteristic band for the pure PMMA is observed at 1721 cm^{-1} which corresponds to the C=O stretching band. The vibrations due to deformation modes of CH$_3$ groups appear at 1489 cm^{-1}, 1434 cm^{-1} and 1385 cm^{-1}. Medium bands at 1268 cm^{-1} and 1238 cm^{-1} indicate the presence of C–O stretching modes. The band at 1189 cm^{-1} is assigned to CH$_3$ wagging mode while the two bands at 1141 cm^{-1} and 1062 cm^{-1} are due to the CH$_3$ twisting.

Figure 4 curve (b) shows the FTIR spectrum of PMMA/0.5 wt% MWCNTs composite. The observed vibration modes due to C–C stretching appear at 985 cm^{-1} and 969 cm^{-1}. The peaks at 912 cm^{-1} and 840 cm^{-1} are assigned to CH$_2$ rocking while the peaks at 809 and 749 are due to the C=O in the plane and out-of-plane bending, respectively. The C–H stretching vibration, which might be associated with the carbon of ethylene, is between 2850 and 3000 cm^{-1}. The peak at 1728 cm^{-1} is assigned to the COO. The relative intensity of the hydrogen-bonded carbonyl group at 1815 cm^{-1} increased with the MWCNTs content. The number of hydrogen atoms in the O–CH$_3$ groups of the composite film remained constant. The intensity of the carbonyl molecular group peaks increased when MWCNTs were added to PMMA. The covalent interaction and hydrogen bonds between PMMA and MWCNTs are desired to inhibit phase separation.

Figure 5a, b, c show the SEM micrographs of the composites with 0.1, 0.3, and 0.5 wt% MWCNTs loading, respectively. Accordingly, the grains have a hemispherical shape with an average size between 6.5 and 13.5 µm. The MWCNTs (the bright spots) were present as small clusters whose distribution was fairly uniform. As the MWCNTs ratio increased, dispersion worsened and large agglomerates were observed at 0.5 wt% MWCNTs loading.

According to Table 1 and Fig. 6, pure PMMA is very brittle with a tensile strength of 8.16 MPa and elongation of $\sim$ 1%. However, addition of 0.1 wt% MWCNTs raised
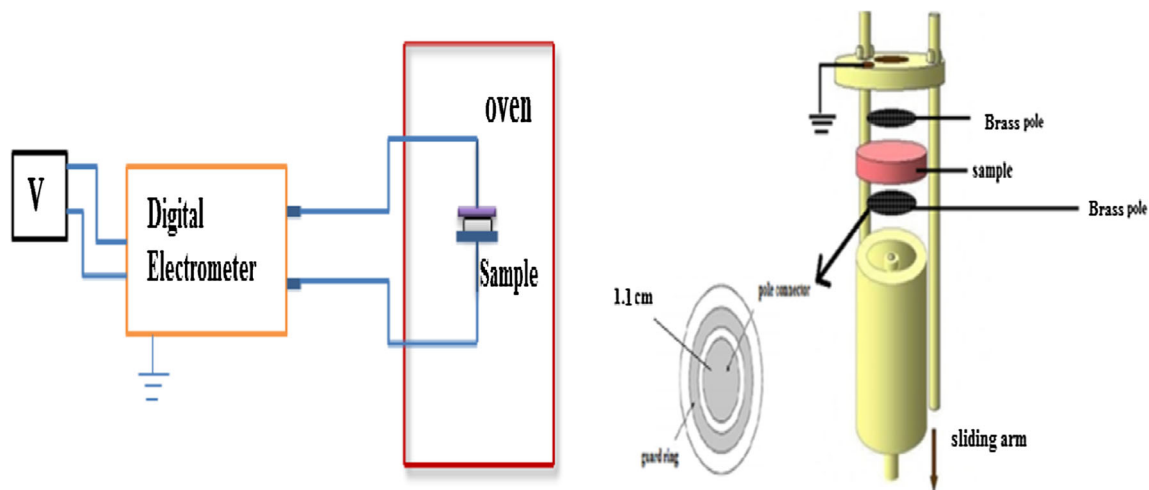
Fig. 3 Schematic diagram of the electrical circuit (left-hand side) used for the dc resistivity measurement. The sample holder and electrodes are depicted on the right-hand side
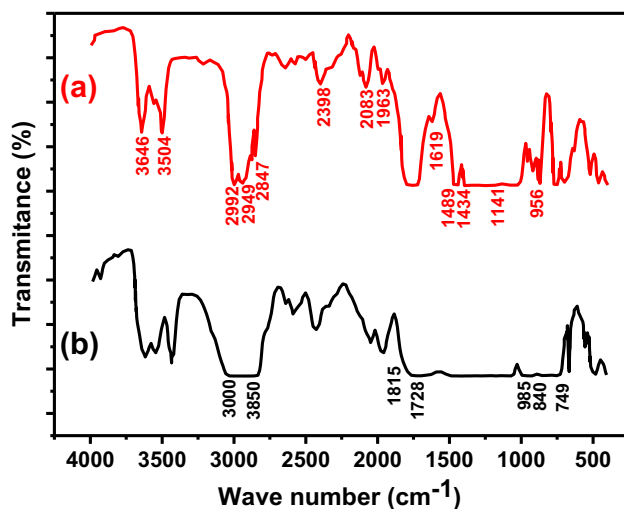

Fig. 4 FTIR of (**a**) pure PMMA and (**b**) PMMA + 0.5 wt% MWCNTs composites

the tensile strength, elongation, Young modulus, tear strength, and hardness by 269%, 88%, 96%, 20%, and 10%, respectively. At 0.5 wt% MWCNTs, the tensile strength, elongation, tear strength, and hardness increased by 397%, 567%, 89%, and 27%, respectively, whereas Young modulus decreased by 26% compared to the PMMA sample. The results obtained for 0.1 wt% MWCNTs composite clearly illustrate the importance of good MWCNTs dispersion at low volume fractions. It also shows that effective reinforcement is limited by the maximum achievable volume fraction where good dispersion can be maintained. Mechanical properties have shown an increase in all the parameters investigated for a low content of carbon nanotubes. The calculated F.E. and I.S. for the composites are given in Table 1. The I.S. increased from 5.96 to 8.12 kg/m^2 while the F.E. fluctuates between 0.16 and 0.19 J as the concentration of the filler increased from 0 to 0.5 wt%, respectively. The maximum and minimum fracture energy were obtained at 0.5 wt% and 0.3 wt% MWCNTs, respectively.

It has been established that surface modification improves MWCNTs dispersion and filler/matrix interfacial bonding. Hydrogen bonds provide important interfacial forces in the composite system. This bond can be intramolecular and intermolecular (such as OH–OH and OH–COOH). Carbonyl groups, available in polymer macromolecules, strongly accept hydrogen to form hydrogen bonds which consequently enhanced the Young modulus of the composites. The increase in tear strength with increased MWCNTs content (Table 1) can be attributed to high tensile strength and Young's modulus of the filler. The strength of the C–C in-plane bonds along the cylinder axis provides strong resistance to any failure including large out-of-plane distortion.

Furthermore, the hardness of the composites increased with MWCNTs (Table 1) which is associated with the uniform dispersion of the fillers within the PMMA matrix. The MWCNTs have a high aspect ratio, high modulus, and high strength, and the loading force can be transferred to the nanotubes. The load transfer also depends on the mechanism of interfacial shear stress between the fiber and the matrix, which can be micromechanical interlocking, chemical bonding, and Van Der Waals force (Du et al. 2007). In addition, MWCNTs raised the Young Modulus of the composites from 7.85 to 16.35 MPa at 0.3 wt% loading. Usually, a higher concentration of MWCNTs leads to a higher Young modulus, for example, ∼ 1 GPa reported by Makireddi et al. (2015) at 10 wt% MWCNT and 4 GPa reported by Jindal et al. (2015) at 5 wt% MWCNTs. The large difference in the moduli could be

Fig. 5 Top-view SEM micrographs of PMMA/MWCNTs composites at **a** 0.1 wt% **b** 0.3 wt% and **c** 0.5 wt% MWCNTs
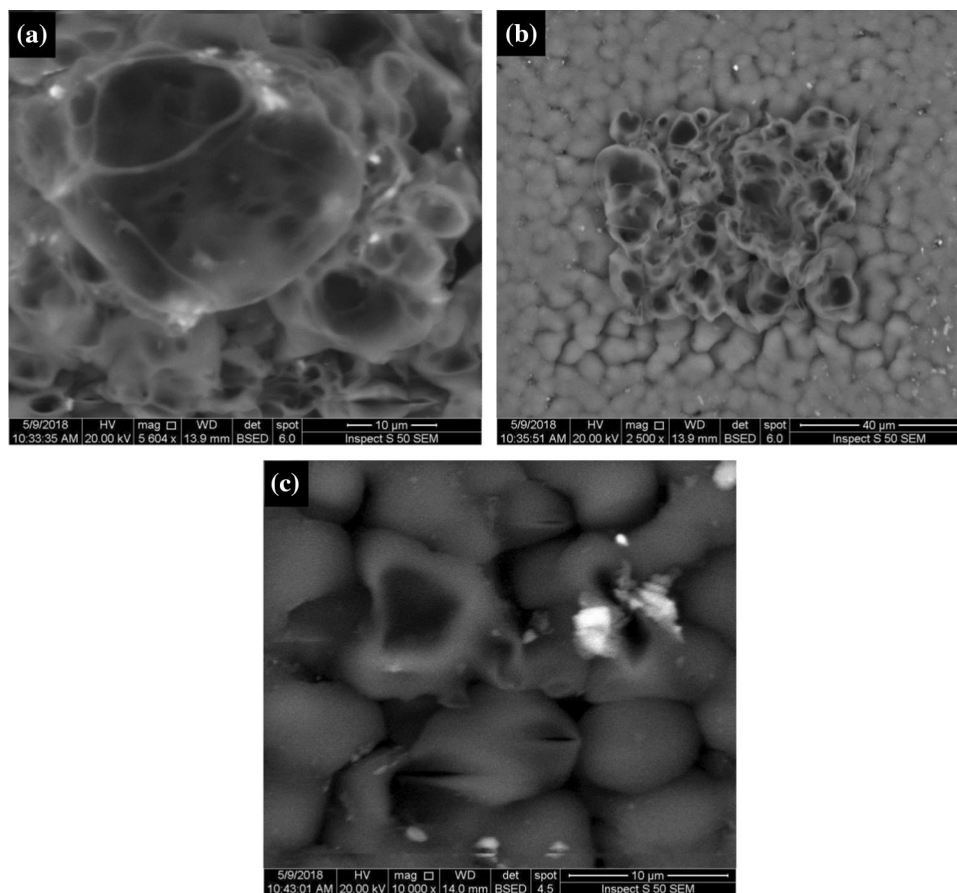

Table 1 Mechanical properties of PMMA and PMMA/MWCNTs composites

MWCNTs Content (wt%)	Tensile Strength (MPa)	Elongation (%)	Young Modulus (MPa)	Tear Strength (mN/mm)	Hardness (Shore D)	Fracture Energy (J)	Impact strength (kg/m^2)
0	8.16	1.04	7.85	10.5	49 ± 5	0.17	5.964
0.1	30.11	1.96	15.36	12.6	54 ± 3	0.18	6.666
0.3	30.99	4.72	6.57	15.3	56 ± 2	0.16	7.24
0.5	40.52	6.94	5.84	19.8	62 ± 4	0.19	8.12

attributed to MWCNTs concentration as well as the diameter of the fillers which lied in the range of 5–15 nm for the present study and 40–60 nm used elsewhere (Makireddi et al. 2015).

The highest tensile strength of 40.52 MPa was obtained at 0.5 wt% MWCNTs compared to 8.16 MPa observed for the control. This is close to 55.6 MPa for the same composition reported elsewhere (Deep and Mishra 2018) as well as the result of Jia et al. (1999). However, the Young modulus in the present study is lower than 100 MPa obtained for PMMA functionalized graphene/polyvinylidene fluoride nanocomposites (Layek et al. 2010). This high value buttresses the point that functionalized surfaces enhance mechanical properties. The effects of

concentration of MWCNTs below 0.1 wt%, aspect ratio, and interfaces miscibility on the mechanical properties of PMMA/MWCNTs composites have been reported elsewhere (Kim and Jo 2008; Mu et al. 2018; Mammeri et al. 2012).

The behavior of σ_{dc} for PMMA/MWCNTs composites as a function of MWCNTs concentrations and temperature is presented in Fig. 7. The increase in σ_{dc} with temperature is similar to the behavior of semiconductors. At room temperature, the σ_{dc} has a value of 2.45×10^{-10} S cm^{-1} reveals the insulating behavior of the PMMA polymer. However, σ_{dc} rose to 2.1×10^{-8}, 7.54×10^{-5} and 1.33×10^{-4} S cm^{-1} for 0.1, 0.3 and 0.5 wt% MWCNTs loading, respectively. The magnitude of σ_{dc} at 0.5 wt%
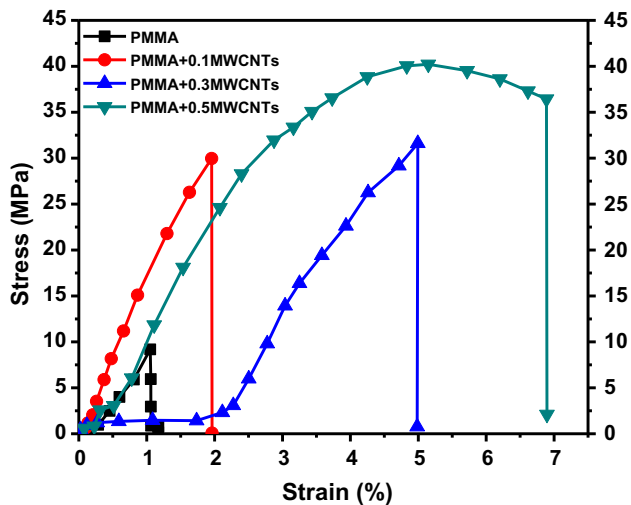
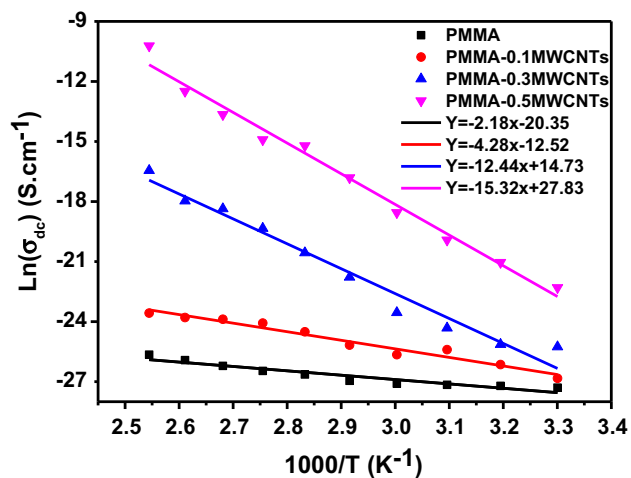**Fig. 6** Stress-strain curves of pure PMMA and PMMA/MWCNTs composites

Fig. 7 Plot of $\ln(\sigma_{dc})$ against $(10^3/T)$ for PMMA and PMMA/MWCNTs composites

loading was 6 orders higher than the control. The observed increase in σ_{dc} is due to the increased carrier concentration occasioned by the addition of MWCNTs (Avilés et al. 2019; Mir et al. 2016; Chayad et al. 2015). The presence of MWCNTs as fillers in the PMMA matrix creates extensive conductive networks that facilitate electrons transport in the composite causing current to flow even in the absence of direct contacts between the nanotubes. This mechanism termed the quantum mechanical tunneling effect, allows electrons to move through an insulator between conductive elements (MWCNTs). The MWCNTs network showed a classical percolating network behavior with a low percolation threshold.

The numerical value of E_a was estimated from the slope of the straight lines fitted into the Arrhenius equation (Fig. 7). These values were estimated to be 0.19, 0.37, 1.07

and 1.32 eV for samples containing 0, 0.1, 0.3 and 0.5 wt% MWCNTs, respectively. The increase in the activation energy is in good agreement with published work (Das et al. 2011) and is most likely due to the stress relaxation of polymer chains (Hsu et al. 2017). This behavior can also be due to the reduction in impurity density occasioned by the agglomeration of MWCNTs in the localized states near the valence and conduction bands.

Figure 8 describes the mechanism of mechanical strengthening and electrical conductivity enhancement in the composites. The MWCNTs fillers dispersed randomly within the PMMA matrix which increased in density with the concentration of the fillers (Fig. 8a). The concentration reaches a critical ratio beyond which MWCNTs agglomerated. The significant increase in elongation (Table 1) is due to the strong interfacial interaction between the PMMA matrix and MWCNTs. This facilitates the formation of bridge cracking and prevents premature failure of the composites. The toughening mechanism of the composites can be described in three stages. In the first stage, a tensile load is applied to the composite beyond the elastic limit of the matrix leading to cracking of the matrix. Further propagation of the crack causes crack initiation in the MWCNTs bundles and subsequent bridging (Fig. 8b). In the second stage, the MWCNTs start aligning in the direction of stress thereby enabling the maximum load to be suspended without failure of the fillers. In the third stage, as the tensile load extends beyond the tensile limit of MWCNTs, the crack propagates rapidly within the fillers. Ultimately, most of the MWCNTs are disrupted and failure of the polymer occurs (Fig. 8c).

Furthermore, applying the electrical field at an elevated temperature over the composites leads to alignment of MWCNTs in the direction of the electric field (Fig. 8d–e). The polarization formed a symmetrical and close macro network (Fig. 8f). The fillers gradually congregated into bundles forming conductive networks in the PMMA matrix leading to the observed increase in electric conductivity. At a higher concentration of MWCNTs, the higher connection is expected to increase electric conductivity. Accordingly, addition of MWCNTs converted PMMA from an insulator to a conductive plastic.

Notably, σ_{dc} can be increased sharply for the case of electrical percolation when the concentration of filler exceeds a critical value called the percolation threshold (Pc). The presence of MWCNTs in the insulating PMMA matrix utilized to a continuous network of electrical connections in the insulator matrix. The discontinuity in the electrical property could be explained in terms of the metal filler concentrations via the percolation theory. As a sufficient ratio of conductive filler is loaded into a polymer matrix, the composite transforms from an insulator to a conductor due to the continuous linkages of filler particles.

Fig. 8 Schematic illustration of mechanical strengthening (**a**, **b**, and **c**) and enhancement of electrical properties (**d**, **e**, and **f**) in PMMA/MWCNTs composites
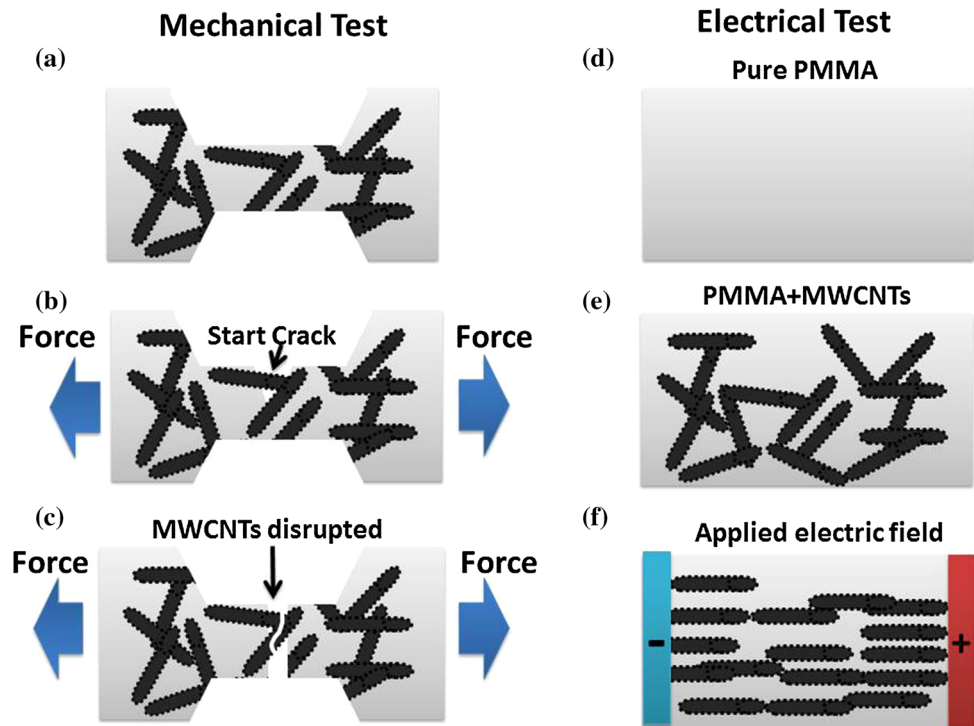
Accordingly, no significant change in σ_{dc} occurs until the Pc of filler loading is reached. For a concentration of conductive filler greater than Pc, the value of σ_{dc} significantly increases due to the formation of a network of chains of conductive particles that span the composite (Sancaktar and Bai 2011). In addition, reducing filler size leads to a decrease in Pc, because inter-particle contacts increase with a rise in the amount of conductive filler (Pothukuchi et al. 2004). Other parameters that can affect the value of Pc are chemical nature of the composite components, preparation method, the crystal structure, thermal and electrical conductivity, dimension, geometry, and distribution of the fillers in the composite (Tee et al. 2007). Although a very large amount of filler is required for conduction, the polymer material's strength and elasticity may be degraded. It is therefore important to use the minimum quantity of conductive filler to achieve the required degree of electrical performance (Li et al. 1993). It can be observed from Fig. 7, the value of σ_{dc} at room temperature at various concentrations of MWCNTs is between 1.4×10^{-12} and 2.1×10^{-10} S/cm. This small change in conductivity reveals that the concentration of conductive filler in the prepared PMMA/MWCNTs composites less than Pc. Therefore, based on the classic theory of percolation, Pc can be obtained by the power-law relationship in polymeric materials by the following equation (Snarskii et al. 2020):

$$\sigma_{dc} = \sigma_0 (P_C - P)^{-q} \text{ for } P_C > P \tag{5}$$

where σ_0 is the conductivity at $q = 0$, P is the concentration of the conductive phase, and q is the critical exponent. The exponent q is the critical exponent and is related to network dimensional aspects. According to Eq. 5, the best linear fitting of $\log(\sigma_{dc})$ versus $\log(P_c - P)$ gives a value of Pc, q and σ_0 at room temperature for PMMA/MWCNTs composites around 0.55 wt%, 2.06, and 4.5×10^{-13} S/cm, respectively. The estimated value of P_C means the concentrations of all prepared samples are less than Pc. In the present study, the value of q is closed to 2 which is normally associated with three-dimensional networks (Snarskii et al. 2020).

4 Conclusion

PMMA/MWCNTs composites were prepared by direct mixing technique while their mechanical and electrical properties were examined at 0.1, 0.3, and 0.5 wt% MWCNTs. The mechanical and electrical properties of the synthesized PMMA/MWCNTs composites were significantly enhanced. For instance, addition of 0.5 wt% MWCNTs enhanced the tensile strength, elongation, tear strength, hardness, fracture energy, and impact strength by 397%, 567%, 89%, 27%, 12%, and 36%, respectively, whereas Young modulus decreased by 26% compared to the control sample. Both the dc electrical conductivity and activation energy were significantly improved. The estimated percolation threshold was found to be $\sim$ 0.55 wt%

MWCNTs. According to FTIR analysis, the carboxyl acid which bonded to the surfaces of MWCNTs strongly influenced dispersion performance. This study demonstrated the huge opportunity embedded in MWCNTs as fillers in composite materials. Moreover, we have proposed a mechanism to simulate the effects of MWCNTs on the electrical and mechanical properties of PMMA/MWCNTs composites.

References

Abd-Elnaiem AM, Hussein SI, Assaedi HS et al (2020) Fabrication and evaluation of structural, thermal, mechanical and optical behavior of epoxy–TEOS/MWCNTs composites for solar cell covering. Polym Bull. https://doi.org/10.1007/s00289-020-03301-5

Aguilar MR, San Román J (2019) Introduction to smart polymers and their applications. In: Smart polymers and their applications, pp 1–11. Woodhead Publishing. https://doi.org/10.1533/9780857097026.1

Arash B, Wang Q, Varadan VK (2014) Mechanical properties of carbon nanotube/polymer composites. Sci Rep 4:6479. https://doi.org/10.1038/srep06479

Ash BJ, Rogers DF, Wiegand CJ, Schadler LS, Siegel RW, Benicewicz BC, Apple T (2002) Mechanical properties of Al₂O₃/polymethylmethacrylate nanocomposites. Polym Compos 23:1014–1025. https://doi.org/10.1002/pc.10497

Avilés F, Oliva AI, Ventura G, May-Pat A, Oliva-Avilés AI (2019) Effect of carbon nanotube length on the piezoresistive response of poly (methyl methacrylate) nanocomposites. Eur Polym J 110:394–402. https://doi.org/10.1016/j.eurpolymj.2018.12.002

Blond D, Valerie B, Manuel R, Kevin PR, Valeria N, Werner JB, Jonathan NC (2006) Enhancement of modulus, strength, and toughness in poly (methyl methacrylate)-based composites by the incorporation of poly (methyl methacrylate)-functionalized nanotubes. Adv Funct Mater 16:1608–1614. https://doi.org/10.1002/adfm.200500855

Chayad FA, Akram RJ, Noor MJ (2015) Effect of MWCNT addition on improving the electrical conductivity and activation energy of electrospun nylon films. Karbala Int J Modern Sci 1:187–193. https://doi.org/10.1016/j.kijoms.2015.10.004

Chen L, Pang XJ, Yu ZL (2007) Study on polycarbonate/multi-walled carbon nanotubes composite produced by melt processing. Mater Sci Eng, A 457:287–291. https://doi.org/10.1016/j.msea.2007.01.107

ASTM D882-18 (2018) Standard test method for tensile properties of thin plastic sheeting, ASTM International, West Conshohocken. www.astm.org. https://doi.org/10.1520/D0882-18

Das M, Ray D, Bandyopadhyay S, Banerjee S, Bandyopadhyay NR, Basumallik A (2011) Thermogravimetric and resistivity study of Ex situ and In situ poly (methyl methacrylate)/carboxylic acid group functionalized multiwall carbon nanotubes composites. J Appl Polym Sci 120:2954–2961. https://doi.org/10.1002/app.33320

Deep N, Mishra P (2018a) Fabrication and characterization of thermally conductive PMMA/MWCNT nanocomposites. Mater Today Proceedings 5:28328–28336. https://doi.org/10.1016/j.matpr.2018.10.117

Deep N, Mishra P (2018b) Evaluation of mechanical properties of functionalized carbon nanotube reinforced PMMA polymer

nanocomposite. Karbala Int J Modern Sci 4:207–215. https://doi.org/10.1016/j.kijoms.2018.02.001

Du J, Bai J, Cheng H (2007) The present status and key problems of carbon nanotube based polymer composites. Express Polym Lett 1:253–273. https://doi.org/10.3144/expresspolymlett.2007.39

Faraguna F, Vidović E, Jukić A (2018) Influence of chemical functionalization of carbon nanotubes on their dispersibility in alkyl methacrylate polymer matrix. J Appl Polym Sci 135:46113. https://doi.org/10.1002/app.46113

Hsu JC, Wenxin C, Fuqian Y, Tsong-Jen Y, Sanboh L (2017) Absorption behavior of poly (methyl methacrylate)–multiwalled carbon nanotube composites: effects of UV irradiation. Phys Chem Chem Phys 19:7359–7369. https://doi.org/10.1039/C6CP08738H

Huang ZM, Zhang YZ, Kotaki M, Ramakrishna S (2003) A review on polymer nanofibers by electrospinning and their applications in nanocomposites. Compos Sci Technol 63:2223–2253. https://doi.org/10.1016/S0266-3538(03)00178-7

Huang YL, Ma CCM, Yuen SM, Chuang CY, Kuan HC, Chiang CL, Wu SY (2011) Effect of maleic anhydride modified MWCNTs on the morphology and dynamic mechanical properties of its PMMA composites. Mater Chem Phys 129:1214–1220. https://doi.org/10.1016/j.matchemphys.2011.06.020

Hussein SI, Abd-Elnaiem AM, Asafa TB, Jaafar HI (2018) Effect of incorporation of conductive fillers on mechanical properties and thermal conductivity of epoxy resin composite. Appl Phys A 124:475. https://doi.org/10.1007/s00339-018-1890-0

Jia Z, Wang Z, Xu C, Liang J, Wei B, Wu D, Zhu S (1999) Study on poly (methyl methacrylate)/carbon nanotube composites. Mater Sci Eng, A 271:395–400. https://doi.org/10.1016/S0921-5093(99)00263-4

Jindal P, Sain M, Kumar N (2015) Mechanical characterization of PMMA/MWCNT composites under static and dynamic loading conditions. Mate Today Proc 2:1364–1372. https://doi.org/10.1016/j.matpr.2015.07.055

Kaufman JG (2001) Fracture resistance of aluminum alloys: notch toughness, tear resistance, and fracture toughness. ASM International. https://trove.nla.gov.au/work/34262925

Khutoryanskiy VV, Georgiou TK (eds) (2018) Temperature-responsive polymers: chemistry, properties, and applications. Wiley. https://doi.org/10.1002/9781119157830

Kim KH, Jo WH (2008) Improvement of tensile properties of poly (methyl methacrylate) by dispersing multi-walled carbon nanotubes functionalized with poly (3-hexylthiophene)-graft-poly (methyl methacrylate). Compos Sci Technol 68:2120–2124. https://doi.org/10.1016/j.compscitech.2008.03.008

Kumar S, Sharma A, Tripathi B, Srivastava S, Agrawal S, Singh M, Awasthi K, Vijay YK (2010) Enhancement of hydrogen gas permeability in electrically aligned MWCNT-PMMA composite membranes. Micron 41:909–914. https://doi.org/10.1016/j.micron.2010.05.016

Landry CJ, Coltrain BK, Brady BK (1992) In situ polymerization of tetraethoxysilane in poly (methyl methacrylate): morphology and dynamic mechanical properties. Polymer 33:1486–1495. https://doi.org/10.1016/0032-3861(92)90126-H

Layek RK, Samanta S, Chatterjee DP, Nandi AK (2010) Physical and mechanical properties of poly (methyl methacrylate)-functionalized graphene/poly (vinylidine fluoride) nanocomposites: piezoelectric β polymorph formation. Polymer 51:5846–5856. https://doi.org/10.1016/j.polymer.2010.09.067

Li L, Lizzul C, Kim HA, Sacolick I, Morris JE (1993) Electrical, structural and processing properties of electrically conductive adhesives. IEEE Trans Compon Hybrids Manuf Technol 16:843–851. https://doi.org/10.1109/33.273683

Logakis E, Pandis C, Pissis P, Pionteck J, Pötschke P (2011) Highly conducting poly (methyl methacrylate)/carbon nanotubes

composites: investigation on their thermal, dynamic-mechanical, electrical and dielectric properties. Compos Sci Technol 71:854–862. https://doi.org/10.1016/j.compscitech.2011.01.029

Makireddi S, Shivaprasad S, Kosuri G, Varghese FV, Balasubramaniam K (2015) Electro-elastic and piezoresistive behavior of flexible MWCNT/PMMA nanocomposite films prepared by solvent casting method for structural health monitoring applications. Compos Sci Technol 118:101–107. https://doi.org/10.1016/j.compscitech.2015.08.014

Mammeri F, Teyssandier J, Connan C, Le Bourhis E, Chehimi MM (2012) Mechanical properties of carbon nanotube–PMMA based hybrid coatings: the importance of surface chemistry. RSC Adv 2:2462–2468. https://doi.org/10.1039/C2RA00937D

Meysami AH, Razavi H, Golpayegani IF, Bagheri V (2017) The effect of volume fraction of single-walled carbon nanotubes on natural frequencies of polymer composite cone-shaped shell made from poly (Methyl Methacrylate). Adv Mater Sci Eng 2017:1–11. https://doi.org/10.1155/2017/7345438

Mir SM, Jafari SH, Khonakdar HA, Krause B, Pötschke P, Qazvini NT (2016) A promising approach to low electrical percolation threshold in PMMA nanocomposites by using MWCNT-PEO predispersions. Mater Des 111:253–262. https://doi.org/10.1016/j.matdes.2016.08.073

Mittal V (2014) Functional polymer nanocomposites with graphene: a review. Macromol Mater Eng 299:906–931. https://doi.org/10.1002/mame.201300394

Mu M, Teblum E, Figiel Ł, Nessim GD, McNally T (2018) Correlation between MWCNT aspect ratio and the mechanical properties of composites of PMMA and MWCNTs. Mater Res Express 5:045305. https://doi.org/10.1088/2053-1591/aab82d

Münker TJAG, Van De Vijfeijken SECM, Mulder CS, Vespasiano V, Becking AG, Kleverlaan CJ, Group C, Dubois L, Karssemakers LHE, Milstein DMJ, Depauw PRAM (2018) Effects of sterilization on the mechanical properties of poly (methyl methacrylate) based personalized medical devices. J Mech Behav Biomed Mater 81:168–172. https://doi.org/10.1016/j.jmbbm.2018.01.033

Nakason C, Pechurai W, Sahakaro K, Kaesaman A (2005) Rheological, mechanical and morphological properties of thermoplastic vulcanizates based on NR-g-PMMA/PMMA blends. Polym Adv Technol 16:592–599. https://doi.org/10.1002/pat.634

Nawar AM, El-Mahalawy AM (2019) Simple processed semi-transparent Schottky diode based on PMMA-MWCNTs nanocomposite for new generation of optoelectronics. Synth Met 255:116102. https://doi.org/10.1016/j.synthmet.2019.116102

Nezakati T, Seifalian A, Tan A, Seifalian AM (2018) Conductive polymers: opportunities and challenges in biomedical applications. Chem Rev 118:6766–6843. https://doi.org/10.1021/acs.chemrev.6b00275

Pahlevanzadeh F, Bakhsheshi-Rad HR, Ismail AF, Aziz M, Chen XB (2019) Development of PMMA-Mon-CNT bone cement with superior mechanical properties and favorable biological properties for use in bone-defect treatment. Mater Lett 240:9–12. https://doi.org/10.1016/j.matlet.2018.12.049

Pothukuchi S, Li Y, Wong CP (2004) Development of a novel polymer–metal nanocomposite obtained through the route of in situ reduction for integral capacitor application. J Appl Polym Sci 93:1531–1538. https://doi.org/10.1002/app.20626

Prasher R, Phelan PE, Bhattacharya P (2006) Effect of aggregation kinetics on the thermal conductivity of nanoscale colloidal solutions (nanofluid). Nano Lett 6:1529–1534. https://doi.org/10.1021/nl060992s

Sancaktar E, Bai L (2011) Electrically conductive epoxy adhesives. Polymers 3:427–466. https://doi.org/10.3390/polym3010427

Snarskii AA, Shamonin M, Yuskevich P (2020) Effective medium theory for the elastic properties of composite materials with various percolation thresholds. Materials 13:1243. https://doi.org/10.3390/ma13051243

Stipho HD (1998) Effect of glass fiber reinforcement on some mechanical properties of autopolymerizing polymethyl methacrylate. J Prosthet Dent 79(5):580–584. https://doi.org/10.1016/s0022-3913(98)70180-5

Su PG, Wang CS (2007) In situ synthesized composite thin films of MWCNTs/PMMA doped with KOH as a resistive humidity sensor. Sensor Actuat B Chem 124:303–308. https://doi.org/10.1016/j.snb.2006.12.034

Tee DI, Mariatti M, See CH, Chong KF (2007) Study on the electrical property of silver (Ag) nanoparticles filled epoxy composites for the application of electrically conductive adhesives (ECAs) in electronic packaging. In: 2006 thirty-first IEEE/CPMT international electronics manufacturing technology symposium, pp 496–505. IEEE. https://doi.org/10.1109/IEMT.2006.4456501

Wang C, Yu B, Fan Y, Ormsby RW, McCarthy HO, Dunne N, Li X (2019) Incorporation of multi-walled carbon nanotubes to PMMA bone cement improves cytocompatibility and osseointegration. Mater Sci Eng, C 103:109823. https://doi.org/10.1016/j.msec.2019.109823

Yuan M, Okamoto K, Bronstein HA, Luscombe CK (2012) Constructing regioregular star poly (3-hexylthiophene) via externally initiated Kumada catalyst-transfer polycondensation. ACS Macro Lett 1:392–395. https://doi.org/10.1021/mz3000368

Yuen SM, Ma CCM, Chuang CY, Yu KC, Wu SY, Yang CC, Wei MH (2008) Effect of processing method on the shielding effectiveness of electromagnetic interference of MWCNT/PMMA composites. Compos Sci Technol 68:963–968. https://doi.org/10.1016/j.compscitech.2007.08.004

Zhang C, Li A, Zhao YH, Bai SL, Zhang YF (2018) Thermal, electrical and mechanical properties of graphene foam filled poly (methyl methacrylate) composite prepared by in situ polymerization. Compos B Eng 135:201–206. https://doi.org/10.1016/j.compositesb.2017.10.026

Zhi CY, Bando Y, Wang WL, Tang CC, Kuwahara H, Golberg D (2008) Mechanical and thermal properties of polymethyl methacrylate-BN nanotube composites. J Nanomater 2008:1–5. https://doi.org/10.1155/2008/642036